WATER SCIENCE SERIES

Integrated Field Investigation of the Upper Bulkley River Groundwater Surface Water Interaction

Jun Yin, Johanna Wick, Ed Bryson, Sam Pittman

June 2026

BRITISH COLUMBIA

No. 2026-01

The **Water Science Series** are scientific technical reports relating to the understanding and management of B.C.'s water resources. The series communicates scientific knowledge gained through water science programs across B.C. government, as well as scientific partners working in collaboration with provincial staff. For additional information visit: http://www2.gov.bc.ca/gov/content/environment/air-land-water/water/water-science-data/water-science-series.

978-1-0399-0186-5

Citation:
Yin, J., J. Wick, E. Bryson, and S. Pittman. 2026. Integrated Field Investigation of the Upper Bulkley River Groundwater Surface Water Interaction. Water Science Series, WSS2026-01. Prov. B.C., Victoria B.C.

Author's Affiliation:
Jun Yin, P.Geo.
Ministry of Water, Land and Resource Stewardship
499 George St., Prince George, BC, V2L 1R5

Johanna Wick, P.Geo.
Ministry of Water, Land and Resource Stewardship
3726 Alfred Street, Smithers, BC V0J 2N0

Ed Bryson, P.Geo.
Ministry of Mining and Critical Minerals
1011 4th Ave, Prince George, BC V2L 3H9

Sam Pittman, RPBio.
College of Applied Biology
#310-1207 Douglas Street, Victoria, BC V8W2E7
(Formerly) Ministry of Forests, Lands and Natural Resources Operation
3726 Alfred Street, Smithers, BC V0J 2N0

Cover Photographs:
Jun Yin

Acknowledgements

The authors would like to acknowledge the Ministry of Forests research portfolio for funding this project. The authors also wish to thank the tremendous field support by many of the water authorization staff in Skeena Region: Abby Morgan, Jelle Faber, Courtney Bridge, and Jason Chiang.

EXECUTIVE SUMMARY

Groundwater and surface water interaction plays crucial roles in managing British Columbia's water resources as one entity. While the concept of hydraulic connectivity links the groundwater withdrawal from aquifers to connected streams, the magnitude of the connectivity is difficult to predict with strong temporal and spatial variabilities of flow paths in aquifers and streams. Desktop analysis without the support of field investigation increases the risk posed by water resource allocation decisions, especially when fish habitats and Environmental Flow Needs (EFN) become the primary concerns.

In this study, we implemented several commonly used field techniques in the Upper Bulkley River watershed to better understand the mechanisms of the hydraulic connectivity at varying scales. These techniques included water level and temperature measurement in wells, water level and temperature measurement in shallow piezometers installed in streambeds and banks, groundwater seepage measurements, and airborne thermal imaging. Most of the field experiments were conducted from 2018 to 2022 with the bulk of the piezometer and seepage metre measurements completed in summer/fall, 2022.

The results of the groundwater level and water temperature measurements in wells corresponded to our understanding of the local aquifer types and their connectivity to surface water bodies. The data collected from shallow wells along the Upper Bulkley River indicates that these aquifers are strongly connected to the stream. In these wells, infiltration often departed from an instantaneous, piston-flow response because of heterogeneity in the vadose zone and vegetation water uptake. As a result, short-term changes in groundwater levels due to precipitation were minimal. Groundwater in deep wells, including those completed in bedrock aquifers, had a much longer residence time and showed no signs of connection with surface water bodies. Shallow groundwater and seepage measurements revealed the complexity of the groundwater and surface water exchange at stream reach scale. During the low flow season when the experiment was conducted, the data show the Upper Bulkley River received ongoing groundwater seepage from shallow aquifers. The magnitude of the seepage varied not only between the two monitoring sites, but also within the same site seasonally. Seepage data were used to calculate streambed hydraulic conductivity, a key parameter that controls the rate of the groundwater and surface water exchange. The calculated conductivity varied both spatially and temporally but was reasonably determined within one order of magnitude. The airborne thermal imaging preceded the field experiment. Although preliminary, the temperature profile aligned well with field observations, and it highlights its potential to be used in future studies.

CONTENTS

1. INTRODUCTION AND BACKGROUND

1.1 Regulatory Context

The *Water Sustainability Act* (WSA) has been in effect since February 29, 2016 and delivers on the Province of British Columbia's commitments to modernize water laws, regulate groundwater use, and strengthen provincial water management in consideration of growing demands for water and a changing climate. Water managers need a thorough understanding of groundwater resources, existing allocation pressures, the interplay between groundwater and surface water, and Environmental Flow Needs (EFN) to make informed water allocation decisions. As groundwater and surface water interactions are inherently complex, the Ministry of Water, Land and Resource Stewardship has been actively pursuing collaborative projects to fill current knowledge gaps, particularly where water usage has a potential impact on EFN.

1.2 Knowledge Gaps and Opportunities

The Upper Bulkley River watershed near Houston, B.C. is a classic valley fill system composed of both deep, confined glacial fluvial aquifers and shallow, unconfined fluvial sand and gravel aquifers with strong connections between groundwater and surface water, especially through the uppermost unconfined fluvial aquifer (Hinnell et al., 2020). There is considerable interest around hydraulic connectivity and EFN in the Upper Bulkley River watershed. This interest is due to the watershed's natural propensity for low flow conditions and reoccurring droughts, its importance as a spawning and rearing area for pacific salmon and steelhead trout, and its importance as a source of water for a variety of users.

2. STUDY FOCUS

2.1 Objectives and Purpose

The Upper Bulkley River Groundwater and Surface Water Interaction Project (UBGIP) is an initiative to increase the understanding of the interaction between surface water and groundwater resources in the Upper Bulkley River watershed near Houston. The intended outcomes of the UBGIP are twofold: 1) strategically collect and synthesize baseline groundwater and surface water data to inform management of the water resources in the watershed; and 2) understand the dynamics of groundwater and surface water interactions at different scales.

The UBGIP continues to fill knowledge gaps related to the following questions:

1. Based on available geological data, what are the extent of aquifers in the Upper Bulkley watershed?
2. Which of the mapped aquifers in the Upper Bulkley River watershed are reasonably likely hydraulically connected to the Upper Bulkley River?
3. What quantity of water does the underlying aquifers contribute to the Upper Bulkley River?
4. What management actions could be undertaken to protect the EFN of the Upper Bulkley River with respect to groundwater allocation?

2.2 General Methodology

To answer the previous questions, government staff utilized both existing datasets available for the study area, as well as new surface and groundwater data collected over several years, mainly from 2020 to 2022.

The existing dataset is comprised of:

- Meteorological data from two weather stations operated by the Province of B.C.
- Streamflow data from the Water Survey of Canada
- Aquifer extents mapped by the Province of B.C.
- Digital Elevation Model (DEM) from Lidar BC

The field dataset is comprised of:

- Groundwater level and temperature data from five private wells, and groundwater level data from one B.C. provincial observation well (OW386)
- Groundwater level and water temperature data from multiple shallow piezometers
- Surface water level and temperature data, and groundwater seepage rate measurements at two locations along the Upper Bulkley River
- Thermal images collected by a drone equipped with a thermal imaging camera

At watershed/aquifer scale, groundwater level trends, especially in response to the climate conditions, are examined using data collected at the wells. At stream reach scale, both shallow groundwater and surface water trends are analyzed in the context of the measured groundwater and surface water exchange. The magnitude and spatial distribution of the exchange are further discussed. The thermal imaging data is preliminary and is discussed largely as a standalone section in this study. It offers useful indications of how future surveys could be refined.

3. DESKTOP STUDY METHODOLOGY

3.1 Study Area

The study area is located within the Interior Plateau physiographic region and is centered on the upper section of the Bulkley River. The town of Houston defines the western boundary while the eastern boundary (approximately between Bulkley Lake and Rose Lake) is situated along a major watershed divide where water flows eastward towards the Fraser River and westward towards the Skeena River. The northern and southern bounds of the study area follow the boundary of the larger Bulkley River watershed (Figure 1).

3.2 Climate

The study area has a continental climate characterized by warm and moist summer and cold winters with extended periods of snow (Nitschke et al., 2012). Based on climate data from 1991 to 2020 and interpolation using PRISM (Parameter-elevation Relationships on Independent Slope Model) (Daly et al., 2008), the calculated mean annual temperature at Topley is 4 ^{0}C, with the warmest month in July at 15.4 ^{0}C and the coldest month in January at -9.4 ^{0}C (ClimateBC_Map, Wang et al., 2016). Mean annual precipitation is 498 mm, among which 184 mm is snow. The highest precipitation occurs in fall (September-November) with 143 mm, and the lowest precipitation occurs during spring months (March to May) with only 84 mm. Future climate projections for the Skeena region suggest warming temperatures of more than 2 ^{0}C in the winter and summer, as well as decreased snowpack and increased moisture variability (Westcott B., 2022).

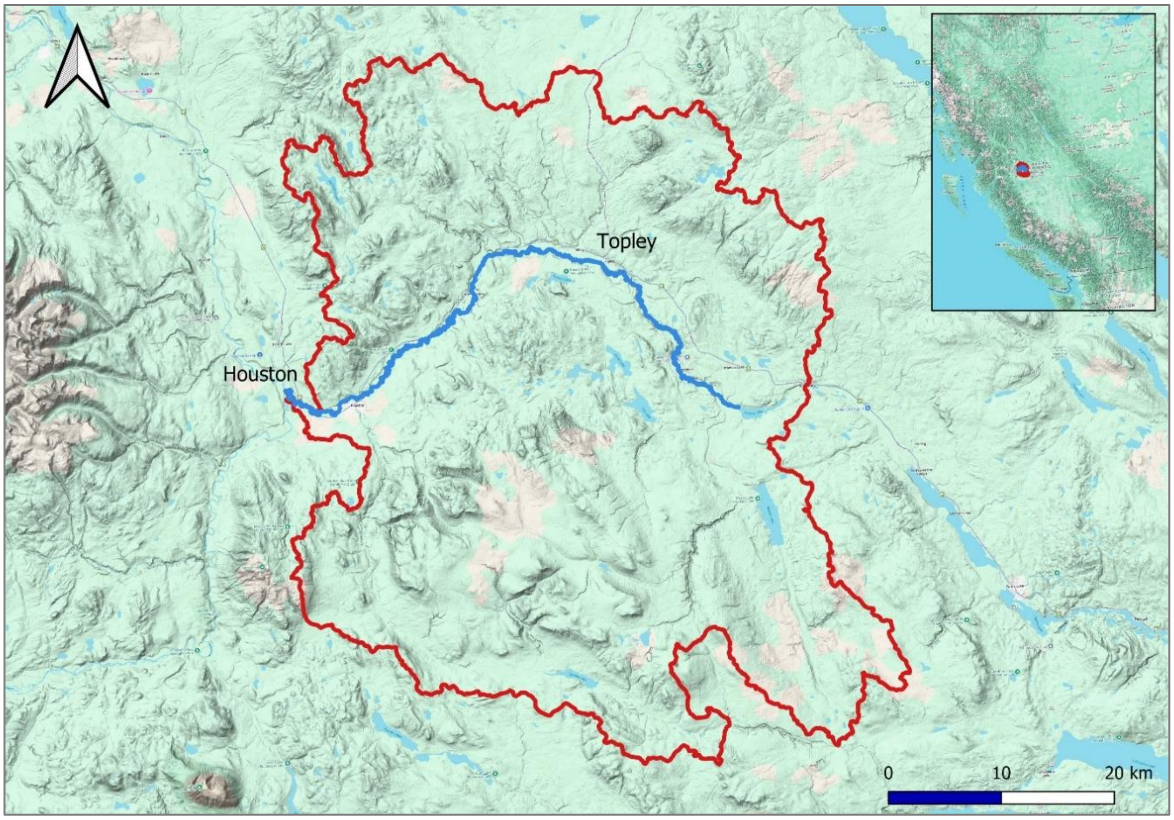

Figure 1: Upper Bulkley River watershed. The centre line of the Upper Bulkley River is coloured in blue.

3.3 Hydrogeology

Aquifers are saturated, permeable geologic formations that can supply usable quantities of water to wells, springs, or streams. Bedrock aquifers in the study area are primarily volcanic units faulted and fractured through the accretion and amalgamation of Intermontane islands and ancient North American continent during the Jurassic Period (Hinnell et al., 2020). Confined unconsolidated aquifers are generally glacial fluvial sand and gravel deposited during the Fraser glaciation, overlaid by fine glaciolacustrine sediment or glacial tills. Post glaciation alluvial, colluvial and organic sediments also form shallow aquifers along the Upper Fraser River (Hinnell et al., 2020).

Within the study area, there are six mapped aquifers. Of these six, two are categorized as unconsolidated sand and gravel aquifers and four as volcanic bedrock aquifers. Five of these six mapped aquifers are interpreted to be confined, with only one as unconfined.

Table 1 below summarizes the information for each aquifer. Copies of the aquifer mapping reports can be found in Hinnell et al., 2020 or through Groundwater Wells and Aquifers (GWELLS).

Two volcanic bedrock aquifers (#658 and #775) are mapped beneath upland sections on the periphery of Houston. Two sand and gravel aquifers (#659 and #660) are mapped beneath the relatively flat lowland section of the Bulkley River valley. The remaining two bedrock aquifers (#652 and #654) are located in upstream areas of the Upper Bulkley River Watershed (Figure 2).

Table 1: Description of aquifers in the Upper Bulkley River watershed.

Aquifer	Location	Type	Size (km^2)	Confined/ Unconfined	No. of wells*	Median depth to water table (m)
652	Northwest of Burns Lake and bordering the southern shorelines of Broman, Old Woman and Conrad Lakes.	Bedrock	4.1	Confined	7	10.67
654	Around the town of Topley	Bedrock	86.8	Confined	13	24.08
658	Around the town of Houston	Bedrock	113	Confined	52	18.29
659	Along the Upper Bulkley River, within the valley bottom	Sand and gravel	40.1	Unconfined	82	3.66
660	Along the Upper Bulkley River, within a valley in the bedrock	Sand and gravel	49	Confined	42	13.72
775	North of the town of Houston, north of the Upper Bulkley River	Bedrock	81.8	Confined	27	41.76

* *This column shows wells that are assigned to this aquifer based on the lithology. It does not include unregistered wells and wells that are not able to be assigned due to lack of information.*

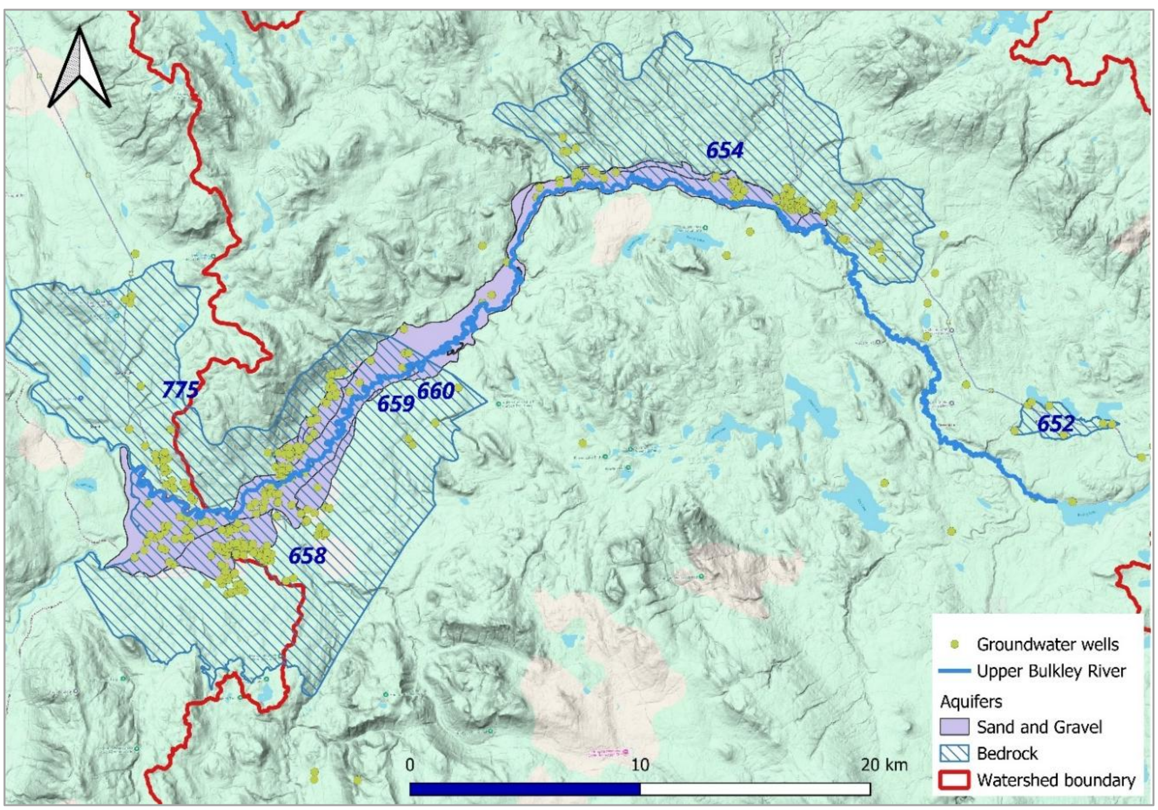

Figure 2: Mapped aquifers and groundwater wells in the Upper Bulkley River watershed.

3.4 Surface Water Hydrology

The Upper Bulkley River originates from Bulkley Lake, flowing northwest and then southwest and joining the larger Morice River where the combined Bulkley River flows north of Houston. Above Bulkley Lake, some tributaries contribute to the lake and are considered part of the Upper Bulkley River's headwater. The river typically experiences one major flow peak caused by the spring snowmelt and several small peaks in fall from precipitation (Figure 3). Summer and winter are low flow seasons with lowest flows typically occurring in late summer due to a combination of low precipitation and increased water usage. There are no established hydrometric stations on the Upper Bulkley River before Houston. One Water Survey of Canada hydrometric station is located on the Upper Bulkley River just above the confluence with the Morice River (Figure 4).

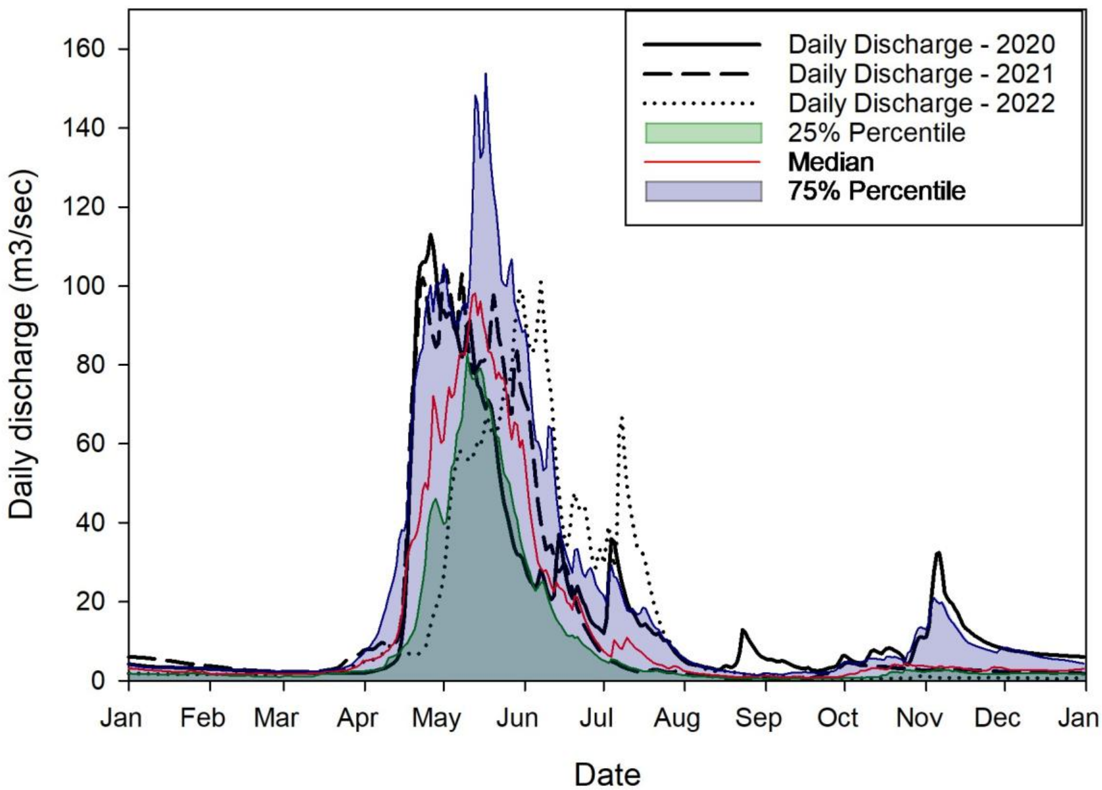

Figure 3: Recorded daily stream flow at Water Survey of Canada's Bulkley River Station (08EE003). The selected data between 2020 and 2022 aligns with the time where most of the field measurements were conducted. Percentiles and median values are calculated based on the recorded data from 2011 to 2022. In each year, one major flow peak occurs in April/May/June resulting from the spring snow melting freshet. Flow recedes to its lowest level at the end summer. Several small peaks (e.g., Nov 2020) are due to fall precipitation events.

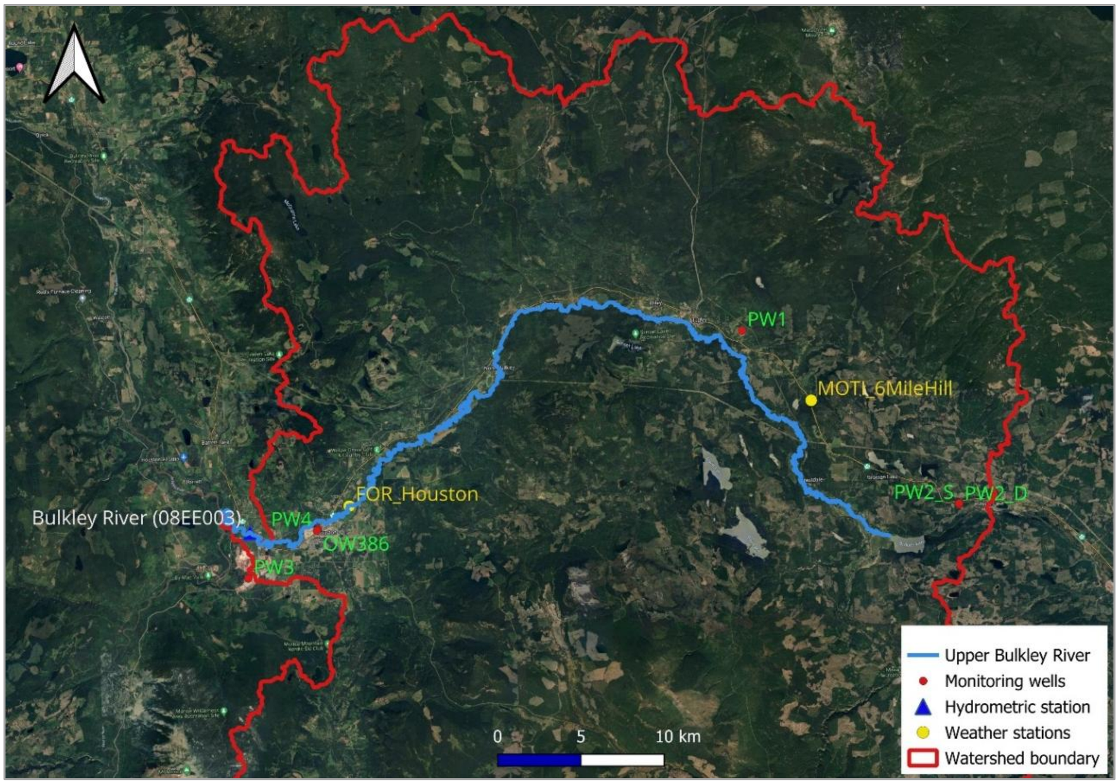

Figure 4: Monitoring stations in the Upper Bulkley River watershed include one hydrometric station, two weather stations, and six monitoring wells.

4. FIELD STUDY METHODOLOGY AND RESULTS

4.1 Precipitation Data

A meteorological station (managed by the Ministry of Forests wildfire management branch, station ID 162) located near Houston (Figure 4) was used as the primary representative weather station for daily accumulated precipitation data. A second meteorological station (managed by the Ministry of Transportation and Transit, station ID 55092) was used to provide more accurate precipitation data for the seepage metre experiment near Topley (discussed below).

4.2 Volunteer Wells

To supplement the one provincial groundwater observation well (OW386) located in the study area, the project team reached out to residents through local newspapers, farmers' markets, social media, and targeted presentations to obtain access to five private wells (Figure 4). Lithology of the volunteer wells was not available, and the associated aquifer was inferred from measured well depth, interpretations of other nearby well logs, and visual inspection of the well construction (e.g., dug or drilled). The associated aquifers and the monitoring period of the volunteer wells are listed in Table 2. To measure groundwater levels and temperature, Solinst Levelogger Edge (M10) were installed in all the volunteer wells. A Solinst Barologger was also installed at each site to record the barometric pressure change for water level compensation.

Recorded groundwater level and water temperature data from the volunteer wells, along with the precipitation during the same period, are plotted in Figure 5 and discussed below.

Table 2: Well-aquifer correlation and the monitoring period of five volunteer wells.

Volunteer Well ID	Aquifer Description	Well Depth (ft) and aquifer material*	Monitoring period
PW1	#660, Bulkley buried channel, confined sand and gravel (S&G) aquifer	107, sand and gravel	2020/9/2 to 2023/6/27
PW2_D	Not mapped (potentially confined unconsolidated, inferred by a nearby well with similar depth)	200	2020/6/29 to 2023/6/27
PW2_S	Not mapped (potentially unconfined or semiconfined unconsolidated, inferred by the shallow depth of the well)	9	2020/6/29 to 2023/3/5
PW3	#659, Upper Bulkley Alluvial, unconfined S&G aquifer	60, gravel	2020/9/4 to 2022/5/25
PW4	#659, Upper Bulkley Alluvial, unconfined S&G aquifer		2020/9/4 to 2022/5/25

** Depth and aquifer material for PW1 was extracted from the well log; depths for PW2_D and PW2_S were from well owner's statement; depth and aquifer material for PW3 was from well owner's statement.*

4.2.1 Volunteer Wells in Confined Aquifers

PW1 is located east of the Village of Topley surrounded by a landscape dominated by agriculture activity. The aquifer mapping report (Hinnell et al., 2020) for Aquifer #660 indicates the overlaying sediments are mainly glaciolacustrine deposits and/or Fraser till. Based on lithology information in the well log, PW1 is confined by 103 ft of advance phase glaciolacustrine deposit (described as "clay silt sand") and glacial till (described as "clay rocks"). This is an active well, and the observed oscillations of water level (up to ~2.5 m daily) were consistent with pumping induced water level change (Figure 5a). Almost all the pumping events were short lived with V-shaped drawdown and recovery. This is interpreted as wellbore storage effects as the pumping duration was insufficient to develop a cone of depression within the aquifer. It is worth noting that in confined aquifers, pore water in the aquifer matrix and water column in a well respond to barometric pressure changes differently. This process is commonly defined as barometric efficiency (e.g., Rasmussen and Crawford, 1997). Many observed small-scale oscillations were possibly caused by the total pressure re-balance between the water in well and water in aquifer pores when rapid barometric pressure change occurred. A detailed assessment of barometric efficiency is challenging because the effects of the barometric pressure were intertwined with concurrent well-pumping influences.

Rapid water temperature oscillations in PW1 are believed to be caused by the heat generated by submersible well pumps. For example, continuous pumping between June 20 and 21, 2023, caused the water temperature to increase by ~0.2 degrees Celsius. The elevated temperature was sustained throughout the pumping period and returned to the background level once pumping ceased. Some of the smaller water temperature increases did not have a corresponding water level change. It is unclear whether all the observed temperature oscillations were caused by heat from the pump or some other influence. Except the series of the short-term pumping effects, the water level and water temperature remain relatively stable, indicating a relatively isolated environment created by the confining sediment. If all of the rapid temperature increases are attributed to anthropogenic effects (e.g., pumping), the natural groundwater temperature would fall within a range of 5.2 °C to 5.3 °C.

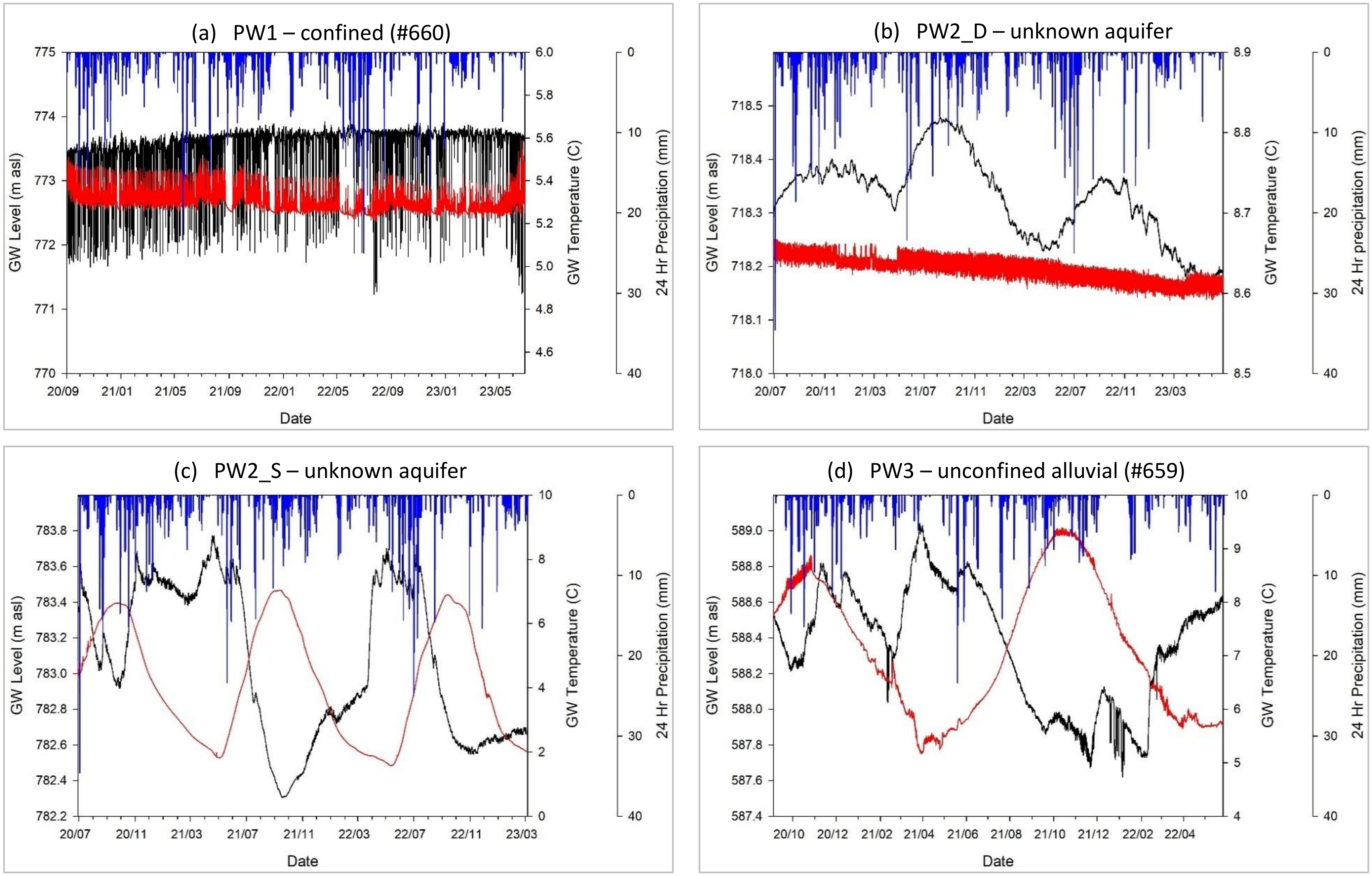

Figure 5: Volunteer well monitoring results: groundwater level (black), water temperature (red), and 24 hr precipitation (blue). Note the differences in measurement periods and vertical scales.

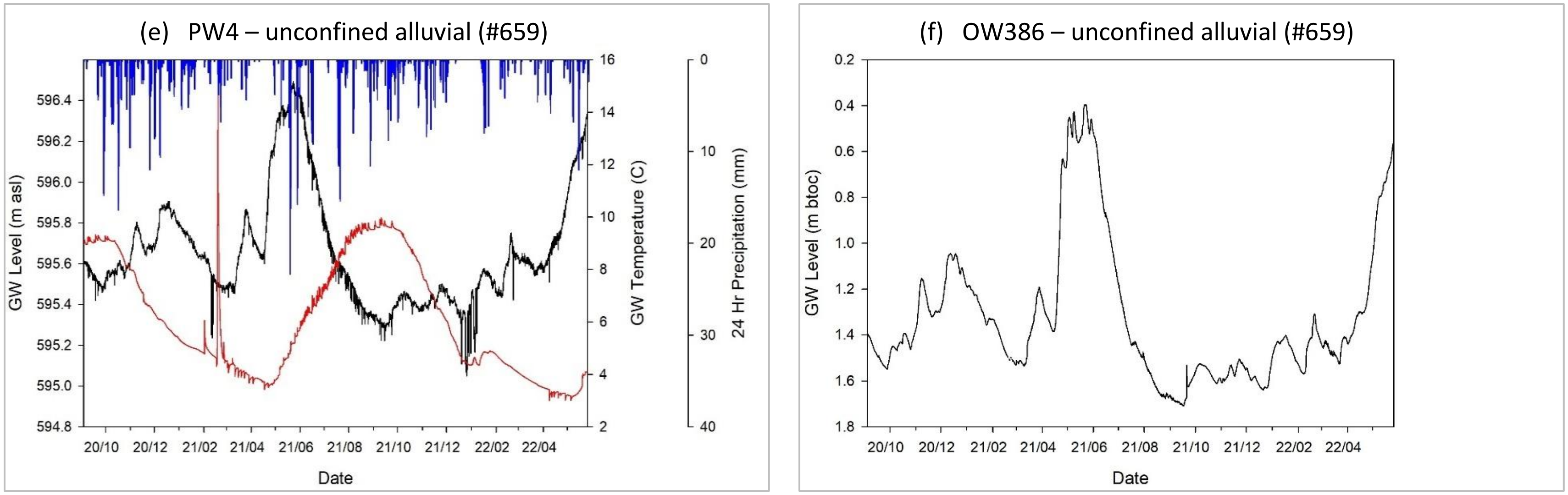

Figure 5 Continued**:** Volunteer well monitoring results: groundwater level (black), water temperature (red), and 24 hr precipitation (blue). Note the differences in measurement periods and vertical scales.

Figure 6: Modifications to volunteer well PW2_D.

PW2_D is an abandoned well buried below the ground surface. The measured well depth was around 200 ft. To facilitate the monitoring, a well cap and PVC conduit were installed when the well was discovered (Figure 6). Because the well was not actively used, the water level was not impacted by in-well pumping and was reflective of natural conditions (Figure 5b). Short-term, small-amplitude oscillations were present through the whole measurement period. These oscillations could neither be correlated to the recorded precipitation, nor to the barometric pressure change. A potential explanation is logger drift. Using a running average smoothing approach with an approximately one-day moving window, the residuals for water level ranged from −1 mm to 1 mm, while temperature residuals ranged from −0.009 °C to 0.008 °C (5%-95% percentiles). These variations are substantially smaller than the stated accuracy of the M10 Levelogger (±5 mm for water level and ±0.05 °C for temperature), indicating the observed fluctuations fall well within the instrument's measurement uncertainty. The prominent water level change was seasonal – water level started to increase in late April/May due to freshet and reached its highest levels in August/September. The magnitude of the water level change is much smaller compared to the water level changes in wells in unconfined aquifers (discussed below). Combined with stable groundwater temperature and the depth of the well, it seems that the source aquifer is partially confined, receiving seasonal recharge through preferential flow paths potentially connected to the nearby surface water bodies (e.g., Bulkley Lake).

4.2.2 Volunteer and Provincial Observation Wells in Unconfined Aquifers

Both PW3 and PW4 are shallow wells completed in alluvial aquifer #659. PW2_S is located further upstream near the headwater of the Upper Bulkley River with a total depth of 9 ft. All three wells displayed similar patterns of seasonal water level and temperature change (Figure 5 c-e). The wells appeared to receive their primary recharge during spring freshet. Groundwater temperature generally decreased during recharge and increased when water levels started to recede at the end of summer. Occasionally excessive precipitation reversed the course of the groundwater hydrograph temporarily (e.g., August 12-13, 2022 in PW2_S, Nov-early Dec. 2021 in PW3). But the overall trends were still very similar to the surface water hydrograph (Figure 3), indicating a strong connection between wells in aquifer #659 and the river. In all three wells, the magnitude of the water level change within a calendar year was around 1.3 m, significantly greater than the water level change in PW2_D (~0.2 m) which also displayed seasonal variability. The effects of pumping on the water levels were visible in all three wells. However, the groundwater temperature profile in PW2_S was much smoother than that in the other two wells, presumably attributable to the nature of the surface mounted pump (e.g., no generated heat) at this site. Because of their proximity, OW386 exhibited a nearly identical hydrograph to PW4.

In general, the measured water level and water temperature in all the private wells and OW386 followed the common understanding of the aquifer recharge mechanism in the region. Deeper confined aquifers have stable water levels and temperatures. Although precipitation may still be the main recharge mechanism, the prolonged infiltration process dampens seasonal signals and regulates the water temperature. Shallow unconfined aquifers not only receive recharge from precipitation but are also heavily affected by changes in surface water levels (e.g., upper Bulkley River and Bulkley Lake). Following all pumping-induced drawdowns, water levels fully recovered, indicating that the aquifers in the region have relatively high transmissivity to support water level recovery.

4.3 In Situ Measurement

Groundwater and surface water interactions occur at different scales (Cardenas, 2015; Woessner, 2020). At stream reach scale, this exchange is often controlled by the hyporheic exchange that are heavily affected by the stream morphology, daily temperature fluctuations, and riparian zone evapotranspiration (Wroblicky et al., 1998; Wondzell, 2006; Gribovszki et al., 2010; Cardenas, 2015). The rate of exchange is also affected by streambed hydraulic conductivity, which is often different than the hydraulic conductivities of the underlying aquifers (Rosenberry and Pitlick, 2009; Rosenberry et al., 2021). Although regional groundwater modeling is a useful tool to address groundwater and surface water exchange quantitatively from a longer term (monthly or yearly) water balance perspective, spatial and temporal variability existing in the hyporheic zone also needs to be examined because it plays an important role on stream temperature and nutrient supply to the aquatic environment (Cardenas, 2015). At the regional scale, Hinnell et al. (2020) examines the static groundwater levels in the watershed and defines the groundwater flow direction (Figure 8B in the report). To better understand the exchange at stream reach scale, piezometers and seepage metres were used to assess exchange rates.

4.3.1 Piezometers and Stilling Wells

Along the mainstream of Upper Bulkley River, three locations were initially selected to test-install the piezometer array and seepage metre in 2021. The installation sites were reduced to two in 2022 due to access issues raised by the property owner at one location. At each location, four piezometers and one accompanying stilling well were installed to co-measure the groundwater and surface water levels, and a seepage metre to directly measure the GW-SW exchange rate. For each piezometer array, two piezometers were installed at the left bank of the stream, one piezometer at the right bank, and one piezometer in the stream channel with the stilling well housed within a PVC pipe attached to the in-stream piezometer pipe. The location and configurations of the two 2022 installations are shown in Figure 7.

To measure water levels, Solinst Levelogger Edge (M10) were installed in both piezometers and stilling wells. A Solinst Barologger was also installed above the water level in one of the bank piezometers to record the barometric pressure change for water level compensation. The loggers were programmed to record water level every 30 minutes. All the loggers were tied to a Kevlar string and were pulled out from the piezometers and stilling wells to download data during site visits. At the beginning and end of each site visit, manual water-level measurements were collected using a water-level tape to recalibrate the logger-recorded water levels. Two elevation surveys were also conducted to ensure that the piezometer pipes had not shifted in the sediments. Table 3 lists the locations of the loggers and measurement periods.

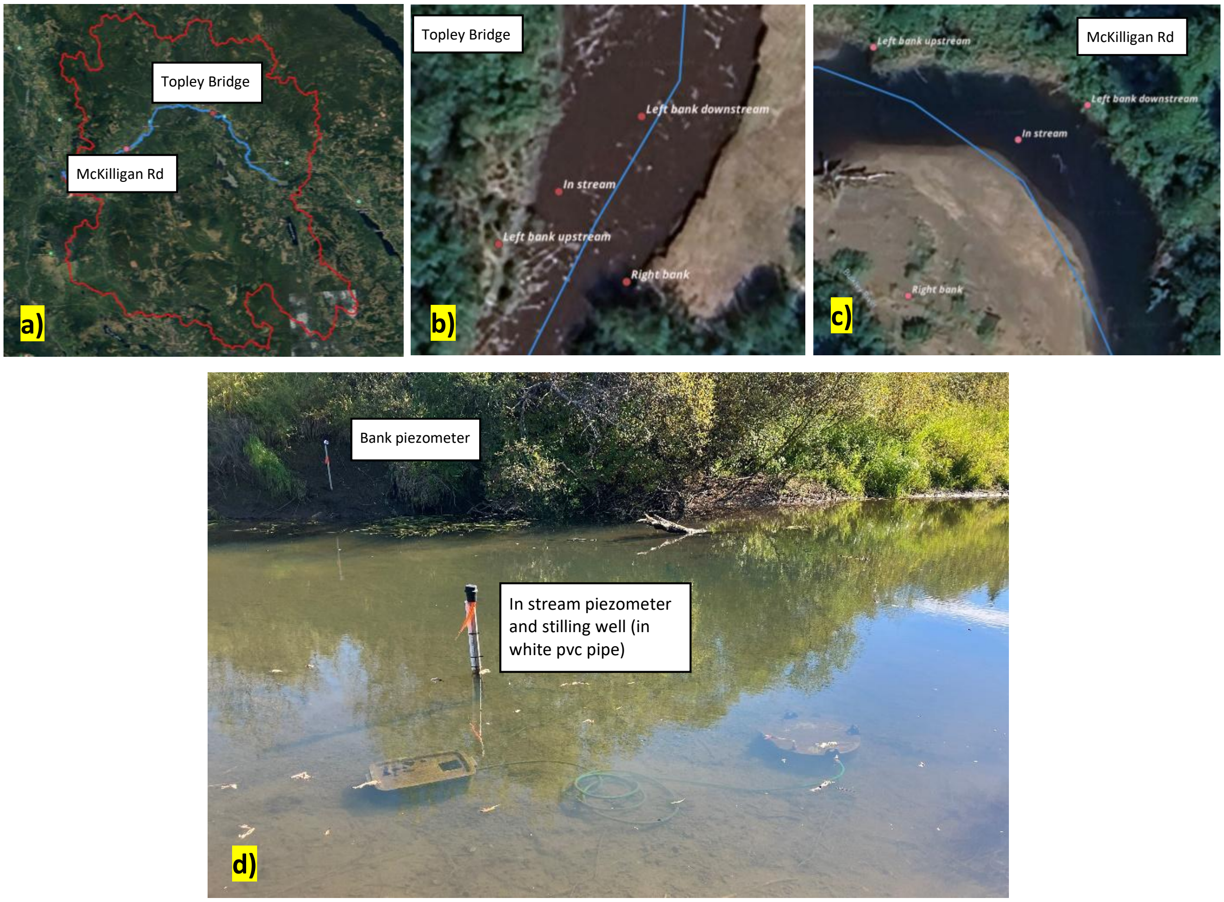

Figure 7: Locations of the two 2022 experiment sites (a), and the arrangement of the piezometer array (b-d). Note the stilling well is attached to the in-stream piezometer pipe. The left bank downstream piezometer at the Topley Bridge site is installed close to the edge of a gravel bar that is under water in the shown satellite image (b).

Table 3: Levelogger information and measurement period at each measurement location.

Site	Logger Location	Measurement Period
McKillingan Rd	Left bank upstream (LB Up)	2022/8/10 to 11/3
	Left bank downstream (LB Down)	2022/8/11 to 11/3
	Instream piezo (In stream)	2022/8/10 to 11/3
	Stilling well (Surface water)	2022/8/10 to 11/3
	Right bank* (RB)	2022/8/31 to 11/3
Topley Bridge**	Left bank upstream (LB Up)	2022/8/11 to 11/3
	Left bank downstream (LB Down)	2022/8/11 to 11/3
	Instream piezo (In stream)	2022/8/10 to 11/3
	Stilling well (Surface water)	2022/8/10 to 11/3
	Right bank (RB)	2022/8/10 to 11/3

* *Right bank piezometer was re-positioned on 2022/08/30.*

** *Barometric pressure measurements at the Topley Bridge site started on 2022/8/24. Barometric pressure measurement from the McKilligan Rd site was used for pressure compensation prior to 8/24.*

4.3.1.1 McKilligan Road Site - Water Level and Temperature Results

At the McKilligan Road site, measured groundwater and surface water temperature (^{0}C) and water elevations (masl) are plotted in Figure 8. The precipitation data was obtained from a weather station (#162 managed by the Ministry of Forests, see Figure 4) to better represent the measurement location.

Surface water temperature recorded in the stilling well displayed diurnal oscillations and decreased when the ambient temperature decreased in late summer and early fall. For the four groundwater locations, two (In stream and RB) showed almost identical temperature signatures. The temperature fell in line with the stream water temperature between the end of August and the beginning of September, during which no significant precipitation was recorded and the water levels dropped to the lowest of the year. At both left bank locations (LB Up & LB Down), however, the up-stream temperature is approximately 10^{0}C higher than the downstream temperature at the beginning of measurements in mid August. Over time, the steady decrease in temperature at the upstream location reduces the temperature discrepancy between LB Up and LB Down. While the overall decreasing trend corresponds with decreases in stream temperature, the absolute temperature remained consistently elevated relative to the stream. This difference is likely attributable to the thermal buffering capacity of the bank sediment, which delays cooling. The same buffering capacity can also explain the lower absolute temperature (compared to the stream temperature) at the beginning of the measurement period. Groundwater contribution to the LB Up location is believed to be minimal.

Although all piezometers were installed to a similar depth below the ground surface, ‘left bank down stream’ is the only location that showed a steady supply of groundwater. Temperature at this location not only remained relatively stable between 6.1 ^{0}C and 8 ^{0}C, but also slightly increased over time contrary to the ambient temperature trends. During the same measurement period from August to early November, PW1 (bedrock aquifer #654) recorded stable groundwater temperature ranging from 5.2 ^{0}C to 5.4 ^{0}C. The groundwater temperature range for PW2_D (unknown unconsolidated aquifer) was between 8.6 ^{0}C and 8.63 ^{0}C, and the groundwater temperature range in PW2_S (unknown unconsolidated aquifer) was between 5.8 ^{0}C and 6.9 ^{0}C. Due to an equipment issue, monitoring in PW3 and PW4 was terminated prior to the installation of piezometers and seepage metres. The “signature” groundwater temperature for different types of aquifers is difficult to determine given that only one or two wells were monitored in each aquifer. However, compared with the other piezometer locations, the LB Down groundwater temperature fell within the range typically observed in wells completed in unconsolidated aquifers.

Despite fluctuations in water elevations, the direction of water level gradients remained stable, with consistently highest water elevations at the LB Up and lowest water elevations in the stilling well. Note that early measurements at the RB were missed (Figure 8b). It is suspected that the initial installation placed the piezometer within a low permeability silt lens that is not well connected to the groundwater system. The piezometer was relocated on August 31, and data presented was collected after that date. LB Down and instream water elevations were roughly equal, falling in between the highest left bank up stream and lowest right bank. Stream elevation at the surface water was lower than all the groundwater elevations recorded at the piezometers.

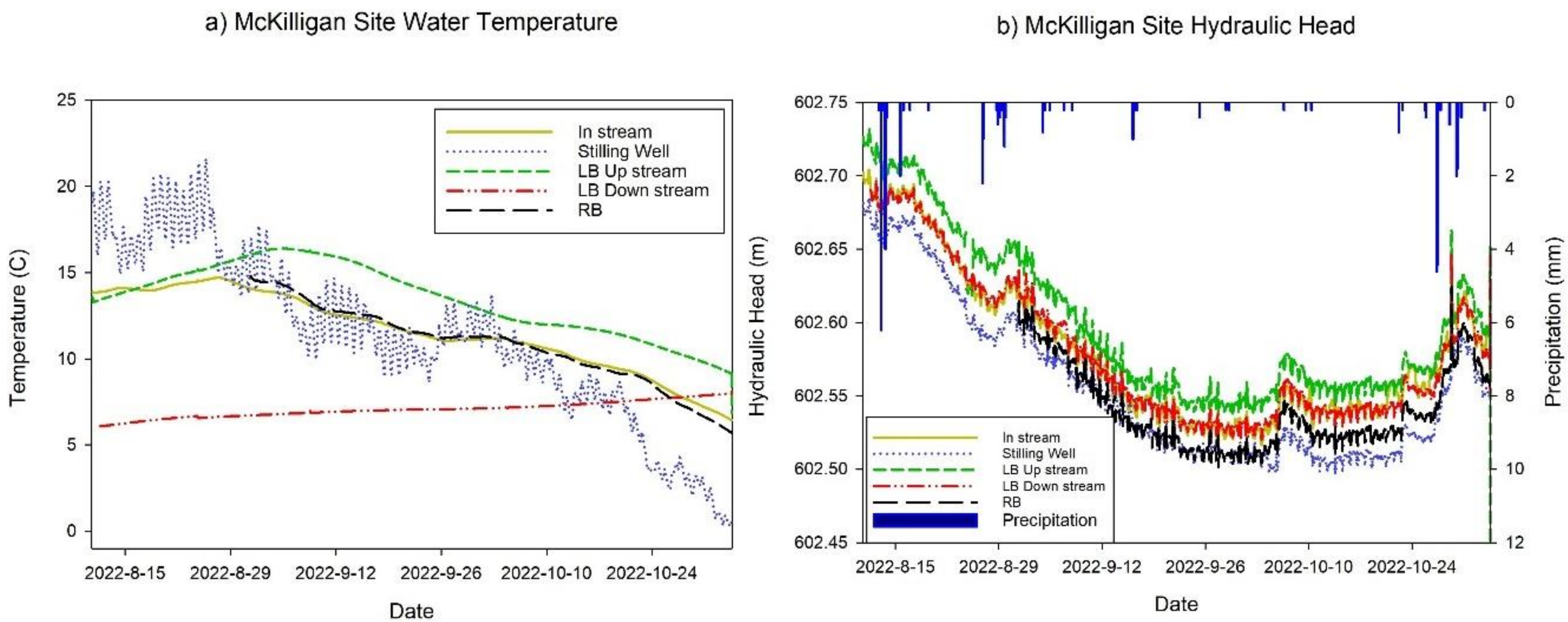

Figure 8: Measured McKilligan Rd site water temperature (a), water elevation and precipitation (b). The right bank measurement started slightly later due to the reinstallation of the piezometer.

Figure 9 shows the high precision Digital Elevation Model (DEM) derived from a 2019 Lidar survey (Lidar BC) and the locations of the piezometers. The DEM map shows that LB Up, in stream, and RB piezometers were all installed within the river channel. There were no bank full occurrences during the time that recordings were being collected. The point bar where the RB piezometer was installed is part of the main channel that could be underwater during the freshet. The LB Down station was installed outside of the river channel, which may explain why this was the only location where groundwater temperatures remained cooler and stable: the other locations were likely located in streambed sediments and highly impacted by the stream water. The inferred groundwater flow direction was generally from the north to south; that is from upstream to downstream, and from left bank to right bank. Lacking the RB high land measurement makes it difficult to determine whether this section of the stream is an entirely flow-through creek. Because this stretch is oriented perpendicular to the main east–west river channel, flow-through conditions are likely. Although groundwater levels on the RB remained slightly higher than the stream water level, the dominant source of groundwater recharge appears to be from the left bank.

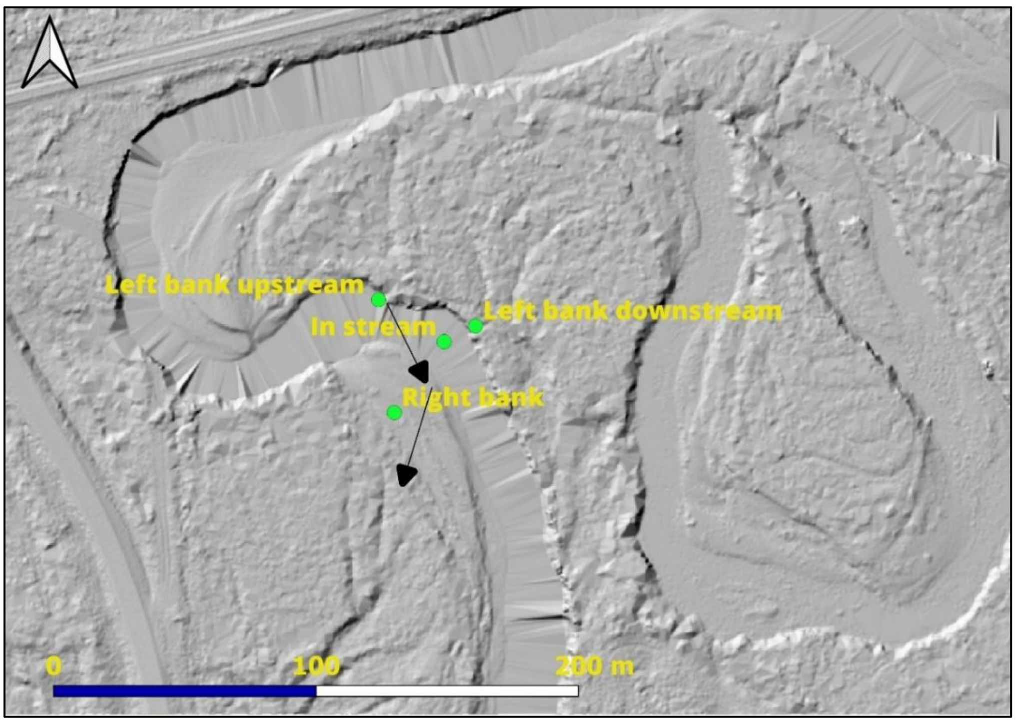

Figure 9: McKilligan Rd site digital elevation model displayed in hillshade, derived from Lidar measurements in 2019 (Lidar BC). The non-vegetated vertical accuracy is 0.1 m. Measurement locations are marked in green dots. Arrows show the inferred groundwater flow directions.

In riparian zones, diurnal change of the shallow groundwater elevation has been documented in previous studies (e.g., Gribovszki et al., 2010; Tian and Xu, 2024). Within the Upper Bulkley River, this change is characterized by water levels decreasing in the morning and rising at night, attributed to riparian vegetation water use. This phenomenon was observed in many rainless days such as 9/25 and 10/17 (Figure 10). The phenomenon became more pronounced at higher ambient temperatures (as reflected by increased stream water temperature in the figure), when vegetation tends to use more water to support elevated transpiration rates. The phenomenon was less apparent on days with precipitation, when vegetation relied less on stream water due to the availability of direct soil moisture inputs. On several other days (e.g., 9/10), when the stream water temperature increased to the highest, a water level “bulge” appeared in the recorded water elevation data during the daytime (Figure 10). These sudden elevation increases may be recording artifacts due to barometric readings that are affected by very high atmospheric temperature (McLaughlin and Cohen, 2011). If this “bulge” is removed, water levels would show decreases in the morning and increases at night, consistent with the riparian water use theory.

4.3.1.2 Topley Bridge Site - Water Level and Temperature Results

Figure 11 shows the measured water temperature (^{0}C) and water elevations (masl) at the Topley Bridge site. The precipitation data was obtained from a different weather station (#55092 managed by the Ministry of Transportation and Transit, see Figure 4).

Of the four groundwater measurement locations, only one site (right bank) showed relatively stable water temperature that appeared unaffected by the stream temperature, ranging from 5.5 ^{0}C to 9.1 ^{0}C. The left bank up and left bank down stream piezometers showed nearly identical temperature profiles, particularly during periods of minimal precipitation. In stream groundwater temperature followed the same trend as both left bank locations but was consistently 2-3 ^{0}C cooler, better aligned with the stream water temperature. This stretch is also oriented perpendicular to the main east–west river channel (Figure 12). If the general groundwater flow direction is from south to north, then both the RB and LB Down piezometers are located in an upgradient position (relative to the stream) and should intersect a groundwater flow signal. But because the LB Down was located at the edge of a gravel bar, its groundwater temperature signal may have been overridden by the stream water, leaving only the RB with a stable groundwater temperature profile.

Water elevation changes over the monitoring period were more dynamic than at the McKilligan Road site. During the first rising limb in August, water elevation at RB was similar to the elevation in stream, followed by LB Up, with LB Down being the lowest (Figure 11b). It seems that groundwater flowed both towards the upstream (LB Up) and downstream (LB Down) perpendicular to the instream and RB direction. Distinguishing whether this reversed flow direction reflects true groundwater movement or simply from measurement uncertainty remains challenging. All water elevations sharply decreased during the first week of September, and the spatial gradient also decreased during this wet-dry transition time. In the second water elevation rising limb from roughly September 8th to October 7th, RB and instream groundwater elevations remained the highest, continuing to drive the groundwater flow to both upstream and downstream directions. But the water elevations at the LB Down increased faster to be higher than the LB Up. From October 7th to the end of the measurement, in stream groundwater level rose to be slightly higher than right bank, and LB Down decreased slightly faster than LB Up and then back to be slightly higher than LB Up. The small gradient changes during this period, and especially the gradient reversals between the RB and instream piezometers, may be attributed, in part, to the errors introduced during data post processing (e.g., the calculation of the position of the leveloggers after each site visit). This increases uncertainty in assessing the direction of groundwater surface exchange after October 7.

The water elevation at the instream piezometer was always higher than the water elevation in the stilling well, indicating that at this location the stream received the groundwater seepage. The seepage was more prominent between September 8th and October 20th, during which the site received the least amount of precipitation. The water elevation differences diminished when multiple precipitation events occurred starting on October 21st.

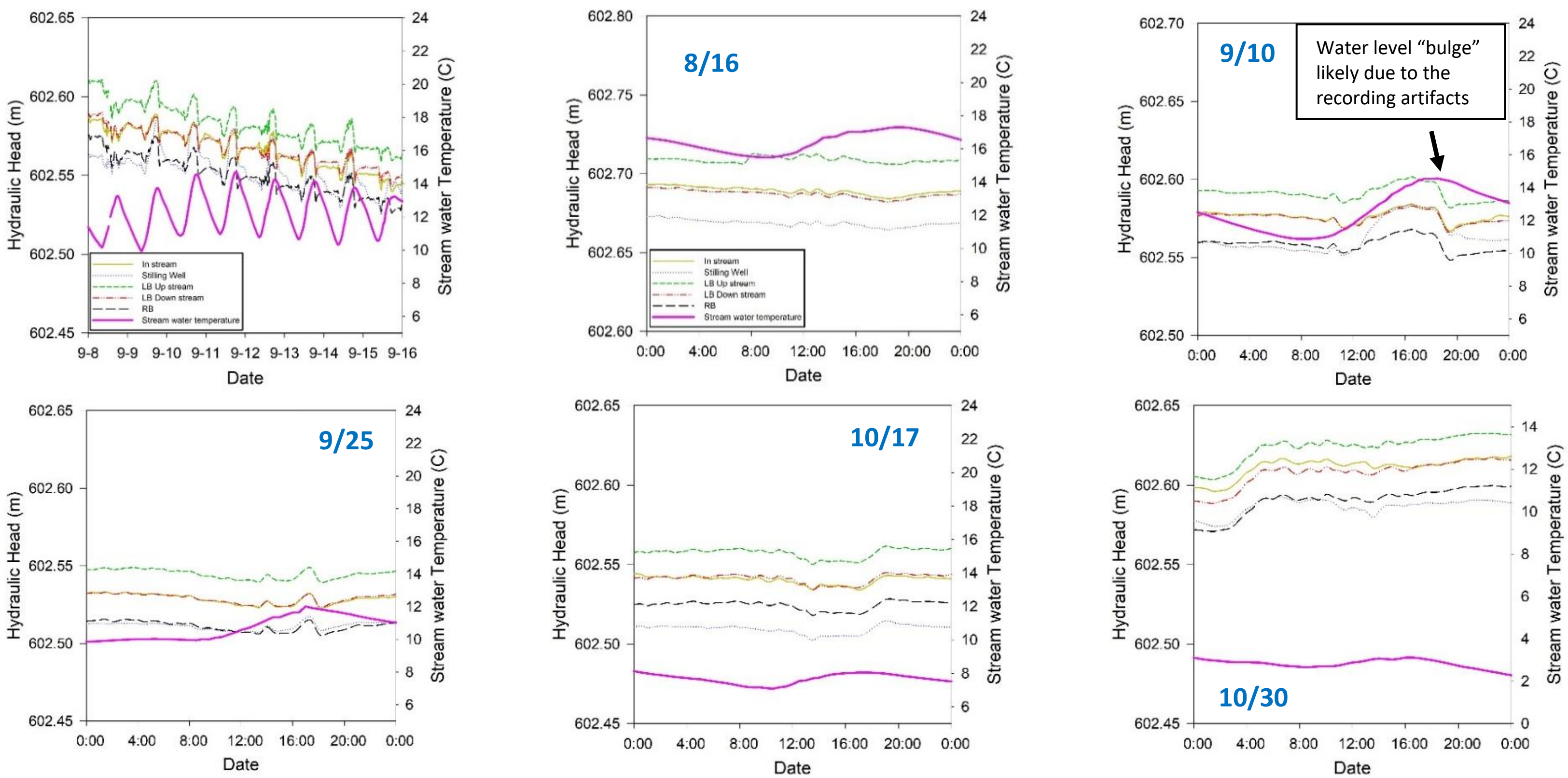

Figure 10: McKilligan Rd site measured water levels showing diurnal fluctuations. Five single days are selected to represent different time periods and weather conditions (e.g., rainless, rain). Within a day, stream water temperature can be regarded as proportional to the ambient air temperature.

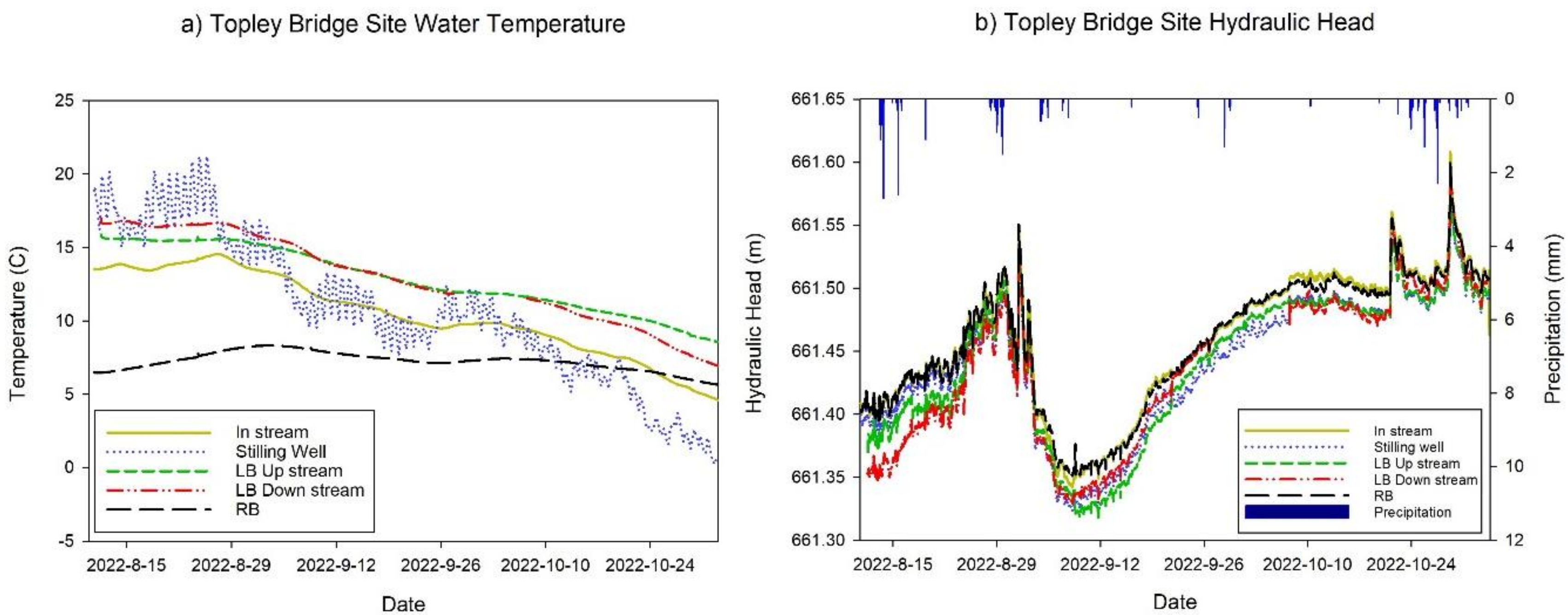

Figure 11: Measured Topley Bridge site water temperature (a), water levels and precipitation (b).

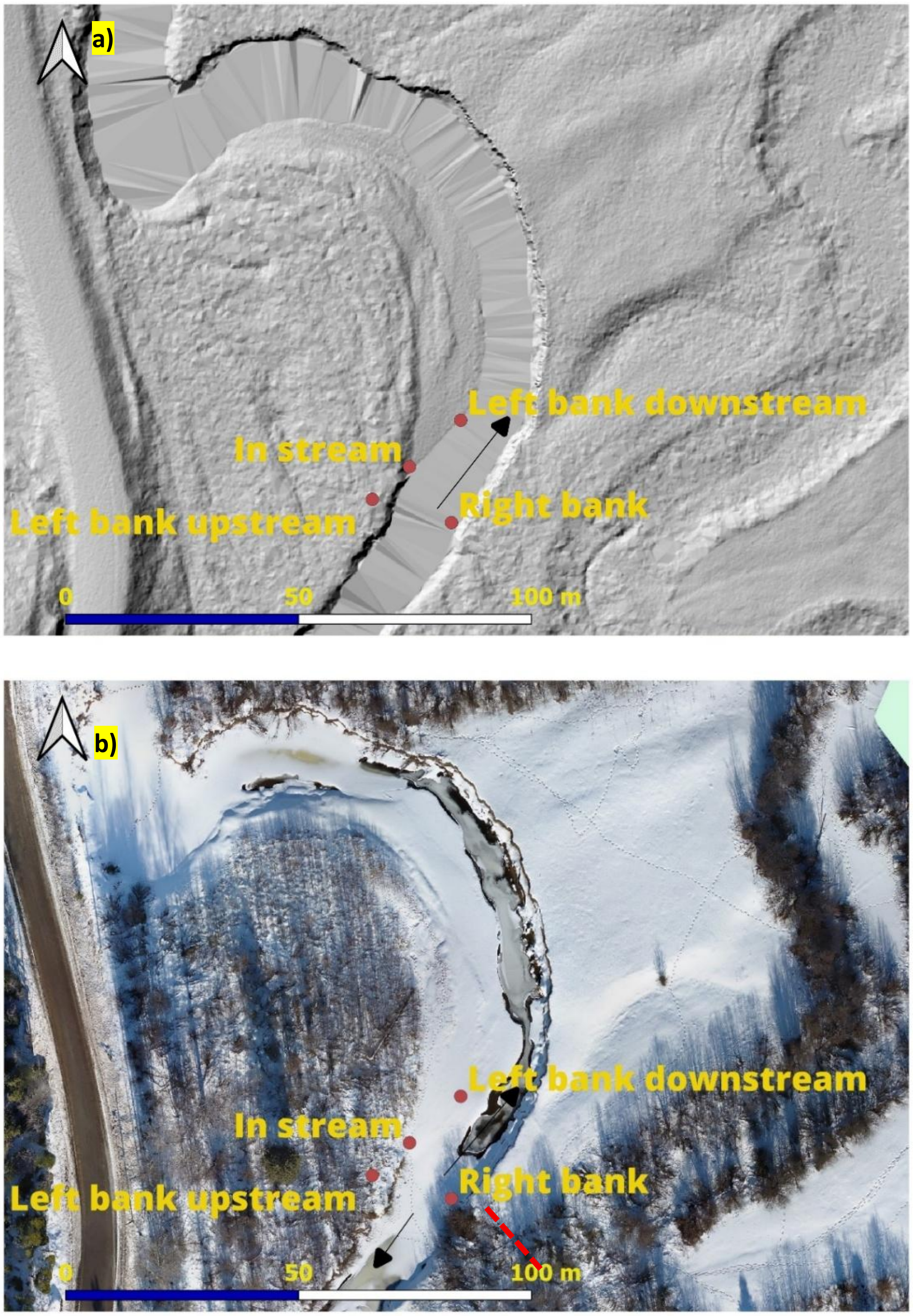

Figure 12: a) Digital elevation model of the Topley Bridge Site displayed in hillshade, derived from Lidar measurements in 2019 (Lidar BC). The non-vegetated vertical accuracy is 0.1 m. Measurement locations are marked in brown dots. Black arrow shows the inferred overall groundwater flow direction; b) Orthomosaic map produced at the same site in February 2022. The red dashed line is where groundwater gradients occur in opposing directions.

Unlike the McKilligan Road site discussed in the previous section, no diurnal water level recession and recovery was observed at the Topley Bridge site (Figure 14), even during periods of no precipitation. Table 4 compares the stream water temperatures on five selected, equally spaced days at both locations. In September, the highest stream water temperature at the Topley Bridge site was around 1.3 ^{0}C lower than the stream temperature at the McKilligan Rd site. Given that both sites consistently received groundwater seepage, and that the groundwater temperature at the Topley Bridge site (7.1 ^{0}C - 9.1 ^{0}C) was slightly higher than the McKilligan Rd site (6.7 ^{0}C - 7.9 ^{0}C) during September and October, the lower stream water temperatures were potentially attributed to shaded conditions at the Topley Bridge site (e.g., higher banks blocking direct sunlight). Furthermore, the Topley Bridge site is closer to the headwaters. It is possible that the stream water was heated along the path when meandering nearly 20 km through the valley to the McKilligan Road site. In addition to the lower temperature, the RB of the Topley Bridge site was mostly cleared for agricultural crop production. The steep cut bank limited the growth of the riparian vegetation that would draw from shallow groundwater (Figure 13). The lower water temperature and lack of riparian vegetation together may explain fewer diurnal oscillations at Topley Bridge site.

Table 4: Daily maximum and minimum stream temperatures at McKilligan Rd and Topley Bridge sites.

Date	McKilligan Rd Max Temp (^{0}C)	McKilligan Rd Min Temp (^{0}C)	Topley Bridge Max Temp (^{0}C)	Topley Bridge Min Temp (^{0}C)
8/16	17.3	15.5	17.2	15.4
9/10	14.6	10.9	13.3	10.1
9/25	12.0	9.9	10.8	9.2
10/17	8.1	7.1	6.7	5.6
10/30	3.1	2.3	2.4	1.4

Figure 13: Riparian vegetation at the cut bank side of the two measurement locations. At the Topley Bridge site, larger and more deeply rooted vegetation had been cleared for crop production.

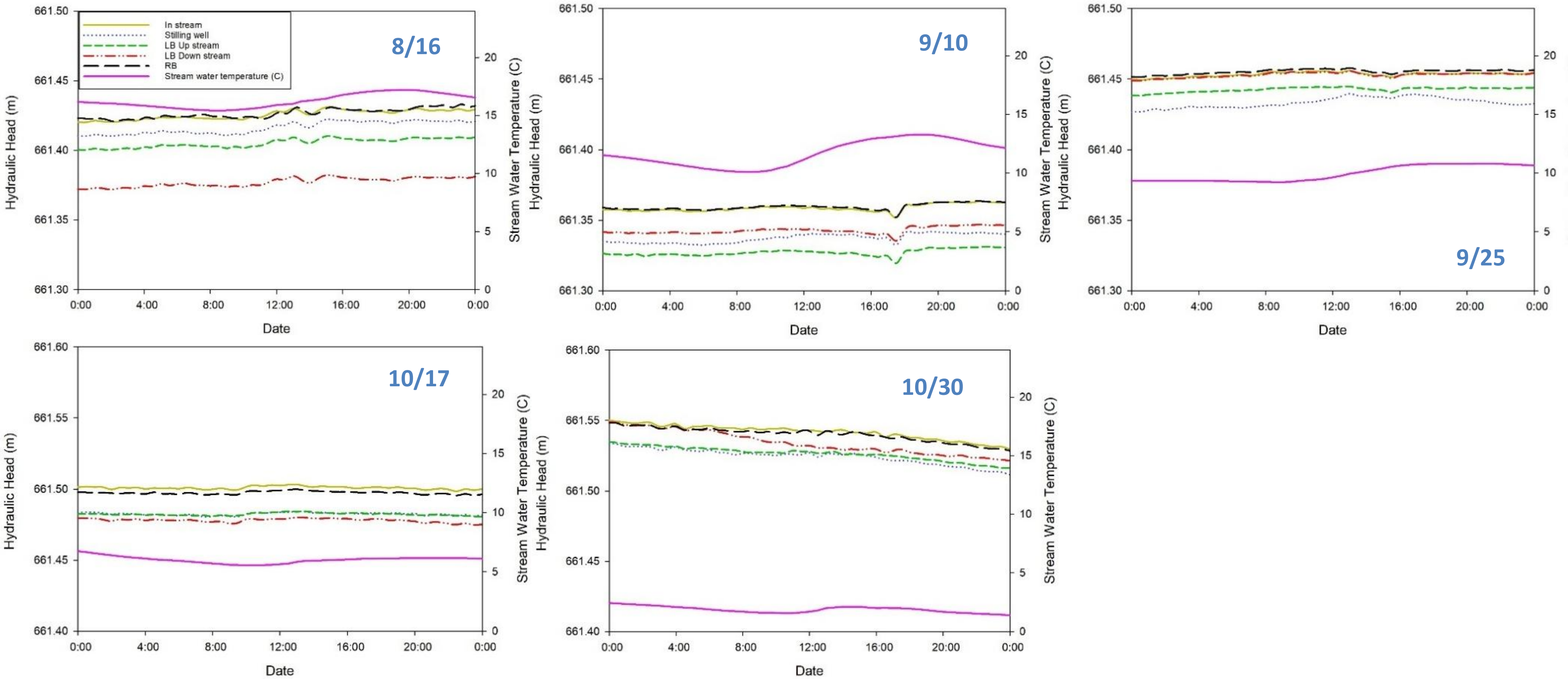

Figure 14: Measured water levels on five representative days spanning the measurement period.

4.3.2 Seepage Metres

At each location, a seepage metre was installed next to the in-stream piezometer and stilling well (Figure 15). The design of the seepage metre followed the basic principles described in Rosenberry et al. (2020). The system included a cylindrical steel drum, a connection garden hose, a collection bag in a protective bag housing, and a connection valve. The cylindrical drums were 65 cm in diameter and 28.6 cm in depth. They had four welded tabs with holes to facilitate the installation (e.g., insert a steel bar to help push and twist the drum). A pre-manufactured spout bag (Nalgene Cantene) was used as the collection bag.

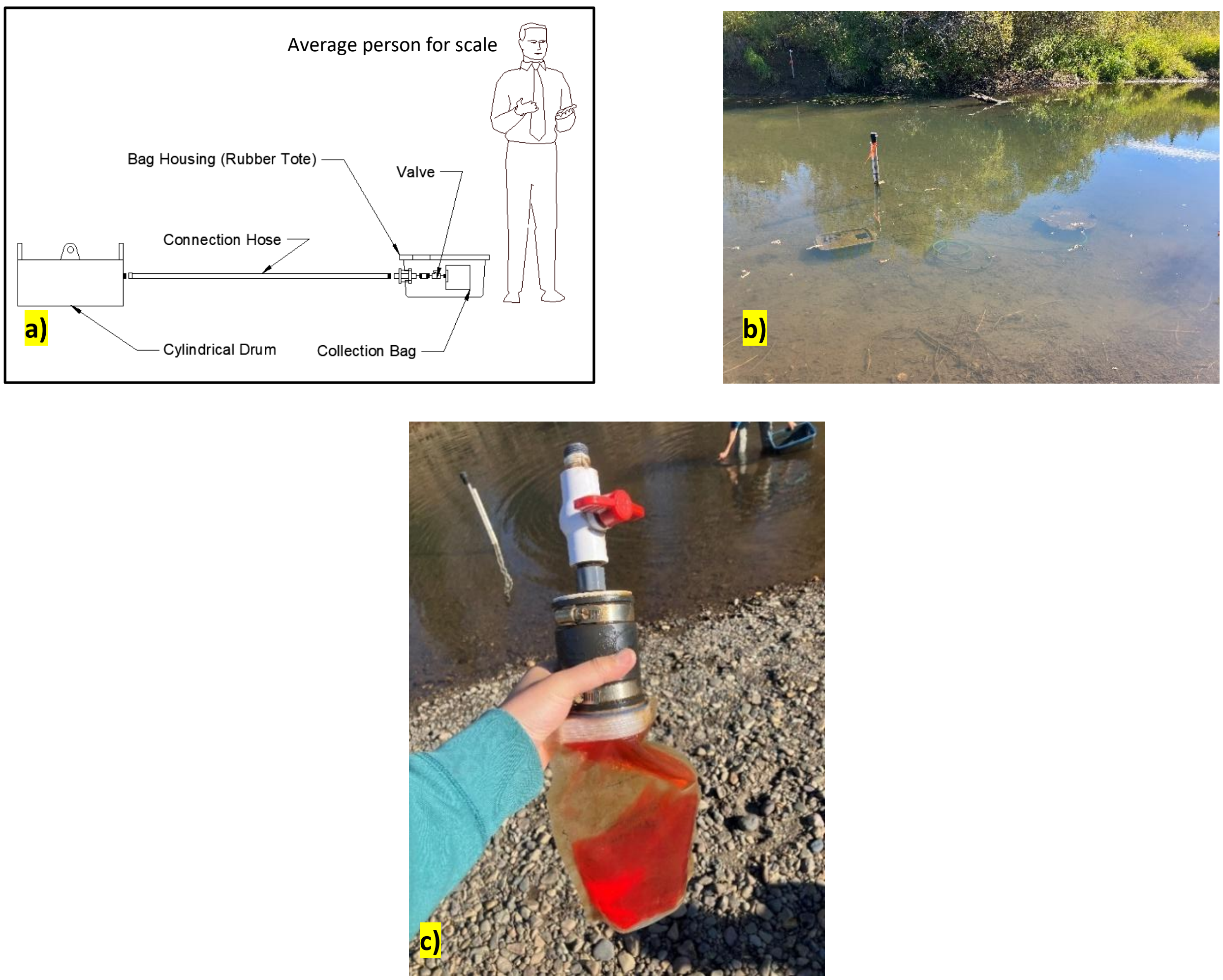

Figure 15: Seepage metre system design (a), field installation (b), and a closer look of the collection bag (c). The food colour was initially added to the water to test for potential leakage and to ensure the free flow of water in the system.

The seepage metre was installed as close as possible to the instream piezometer and stilling well so that the measured water levels would be effectively the same as the water levels at the seepage metre site. To avoid flow induced pressure changes, the cylindrical drum was placed closer to the bank where stream flow is less turbulent. Before installation, any cobbles or large stones were removed to ensure that the edge of the cylindrical drum would not become jammed against them. During installation, the cylindrical drum was pushed at least 8 cm into the riverbed sediment to ensure a proper seal. The collection bag and all the connections were tested with dyed water to identify any leakage and ensure free flow. The bags were filled roughly 1/3 full of water before being deployed to balance the pressure inside and outside of the bag. Rubber storage bins were used as bag housings to protect from flowing water or floating objects. The bin was placed a few feet away from the cylindrical drum to avoid any disturbance at the drum site while disconnecting and connecting the collection bag. The bin was held in place by adding weights on the lid.

Each site was visited about every three days to record the change in weight of the collection bag. To test the potential daily flux dynamics, both sites were visited multiple times on August 31, 2022. During each visit, the valve between the collection bag and the garden hose was closed, and the collecting bag was removed from the bag housing for weighing. During some visits, the hose was found twisted from water flow, or the protection bin had been overturned (potentially by animals). In these cases, after taking the measurements, the collection bags were emptied and refilled to the initial condition. After each weighing, the bag was reconnected back to the garden hose. From August to October, the collection bags were weighted 23 times for the McKilligan site and 24 times for the Topley Bridge site.

4.3.3 Seepage Metre and Groundwater-Surface Water Exchange Rate

Integrated seepage volumes were measured 23 and 24 times at McKilligan Rd site and Topley Bridge site, respectively. The elapsed time between consecutive collections ranged from 113 minutes to 15,986 mins (~11 days). The collection intervals were not pre-set but driven by the availability of field staff. Two to three days were the common collection length. The integrated seepage volume collected by the seepage metre was simply the collection bag weight difference between two successive collections. The seepage rate can be calculated by determining the hydraulic gradient between the groundwater elevation in the in-stream piezometer and surface water elevation in the stilling well:

$$q = K\frac{h_{in}-h_s}{L} \quad (1)$$

$$Q = q \times A \quad (2)$$

Where h_{in} (m) and h_s (m) are the groundwater elevations (hydraulic head) of groundwater (represented by the in-stream piezometer measurement) and surface water (represented by the stilling well measurement), respectively; L (m) is the travel distance between where the groundwater hydraulic head was measured (assumed in the middle point of the screened section of the piezometer) and the stream bed; K (m/min) is the vertical hydraulic conductivity of the streambed sediment; and q (m/min) is the calculated flux. The flux can be converted to the seepage volume (Q) based on the known bottom opening area of the seepage metre cylindrical drum.

The averaged K value between the two consecutive collections can be back calculated using the measured Q. Some previous studies indicated that the vertical K not only has strong spatial variability (Genereux et al., 2008) but also varies temporally at the same location (Rosenberry and Pitlick, 2009; Rosenberry et al., 2021). The variability is more prominent in the fluvial environment, where currents alter grain size distribution and sedimentary structures through dynamic erosion and deposition. In a confined system such as in the enclosed cylindrical drum, K values can also change because the fine material becomes compacted or loosened as the flow direction shifts between downward and upward

(Rosenberry et al., 2021). However, in the current experimental setting, it is difficult to assess whether the seepage rate variabilities can be fully attributed to changing K values. As discussed previously, measured in-stream groundwater elevations were always higher than the measured stream water elevations. Therefore, the collection bags should constantly receive inflow, and all the integrated groundwater seepage (Q) should be positive. However, at the McKilligan Rd site, 9 out of 23 collections were negative, and at the Topley Bridge site, 8 out of 24 collections were negative (Figure 16). The changing K can change the magnitude of the groundwater seepage but not the groundwater flow direction. The negative inflow may suggest that the collection device was impacted by the additional pressure applied to the collection bag (e.g., flowing water into the bag housing), or leakage caused by sediment scouring at the upstream end of the cylindrical drum. Recreational activities were occasionally observed near the collection sites, but their potential impact on the results is difficult to assess.

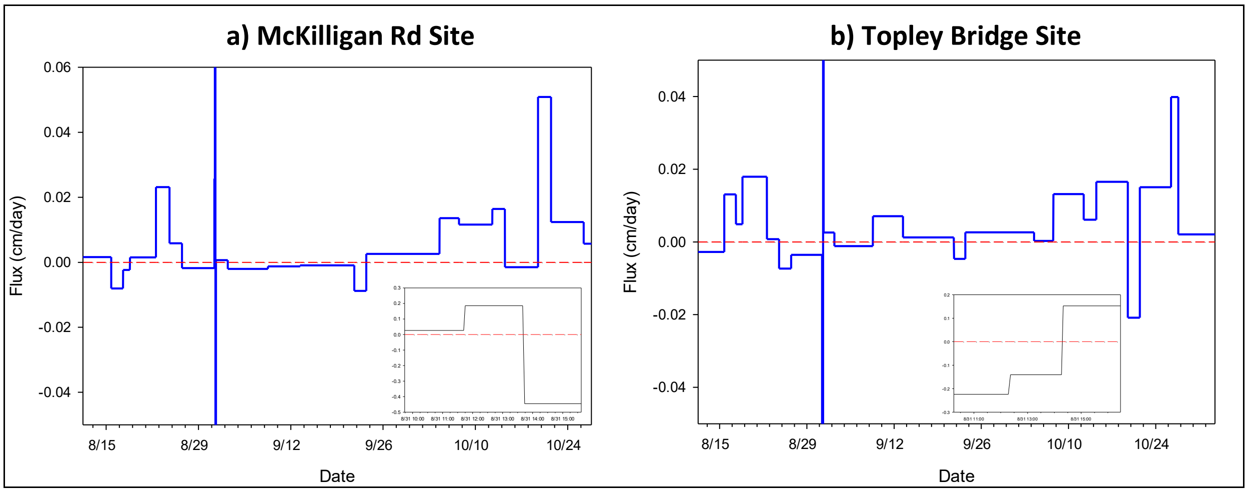

Figure 16: Measured seepage flux at: a) McKilligan Rd site, b) Topley Bridge site. Each horizontal line represents the averaged flux (measured at the end of the collection period) during each collection period. The inserted figure is the measured seepage flux on August 31st when multiple collections were performed.

If K is assumed to remain steady, and the measured hydraulic gradient is correct, the measured and the calculated seepage should follow the 1:1 linear regression line. A trial-and-error approach (increase K by 0.0001 m/min at a time) was used to adjust the K value to assess whether a single, fitted K can be used to reasonably calculate the groundwater seepage to the Upper Bulkley River based on the measured hydraulic gradient. The calibration target was root mean square error (RMSE). Compared with the influx, the negative fluxes were small in magnitude, suggesting either minimal streamflow loss or potential measurement errors. During the calibration, all negative inflow data points were removed to improve the regression. Figure 17 shows the results and the calculated RMSE for both sites.

While some weak correlation exists at the McKilligan Rd site (R^2= 0.212), the calculated seepage rates at the Topley Bridge site (R^2= 0.021) were significantly lower than the measured rates, especially when the measured seepage volumes were over 100 ml. Although this could suggest that the in-situ K increased due to streambed sediment mobilization under higher flux, a lower K value is still required to achieve the overall best model fit. On the other hand, if one assumes that the measured seepage truly represents the groundwater recharge to the river and is used to back calculate K, then at the McKilligan Rd site the K value ranges from 5.3×10^{-9} m/sec to 1.4×10^{-6} m/sec, and at the Topley Bridge site the K value ranges from 1.78×10^{-9} m/sec to 4.27×10^{-7} m/sec. The ranges of K at both sites are within the lower hydraulic conductivity range of silt (1×10^{-9} to 2×10^{-5} m/sec) and higher hydraulic conductivity range of clay (1×10^{-11} to 4.7×10^{-9} m/sec) (Domenico and Schwartz 1990). This is consistent with field observations at both sites, which indicated silty clay or compacted silt is the dominant stream bed material.

At both sites, the difference between most of the calculated K values based on measured seepage (changing K) and the fitted K value (constant K, 5×10^{-8} m/sec for McKilligan Rd site and 3.33×10^{-8} m/sec for Topley bridge site) was within one order of magnitude. The exceptions were both on August 31st, where at the McKilligan Rd site the calculated K is 27 times higher than the fitted K, and at the Topley Bridge site the calculated K is 12 times higher than the fitted K. On August 31st, three seepage collections were conducted at each site to assess the daily variations. We speculate that the larger difference between calculated and fitted K on August 31 is likely associated with the much shorter duration between measurements, which other factors such as short-term streamflow change and evapotranspiration can have significant roles in controlling the seepage volume. We recommend allowing a certain length of time (e.g., more than 24 hrs) between consecutive collections to reduce such uncertainties.

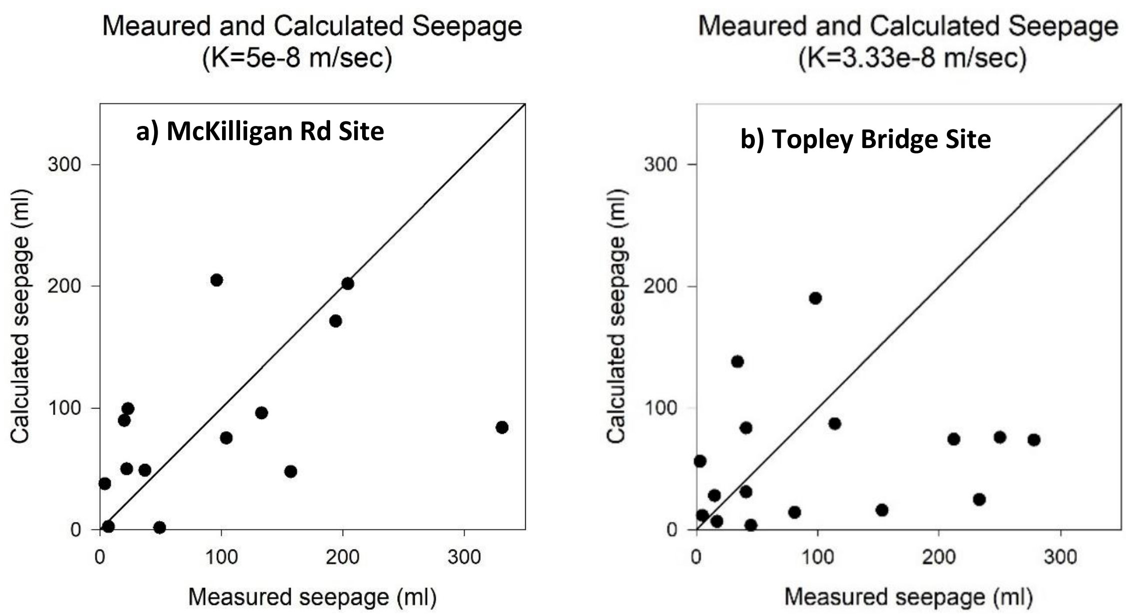

Figure 17: Calculated and measured groundwater seepage (positive only) at: a) McKilligan Rd site (R^2= 0.212, RMSE=85.6 ml); b) Topley Bridge site (R^2= 0.021, RMSE=107.4 ml).

The calculated groundwater seepage (30 mins integration) is plotted in Figure 18 based on the fitted K values. In general, the groundwater seepage rate at the McKilligan Rd site is greater than the rate at the Topley Bridge site. The seepage at this site increased almost 100% entering October when the weather pattern shifted from dry to wet. This is likely due to the lack of vegetation at the site where precipitation quickly infiltrated and returned to the stream in the form of shallow groundwater. At the Topley Bridge site, seepage remained relatively stable similar to the McKilligan Rd site summer rate at 0.3-0.4 ml per 30 mins since late August. It is unclear why the seepage rate prior to late August was a lot smaller. Without surrounding water use information, it is not possible to assess if water use impacted the groundwater recharge.

The total length of the Upper Bukley River down from Bulkley Lake is approximately 98 km. If groundwater flows along the entire reach were roughly approximated by assuming a wetted crosssection of one metre and a uniform rate of 0.3-0.4 cm^3 per 30 mins as the groundwater seepage representative of the driest period of the year, the resulting integrated groundwater fed streamflow in the upper Bulkley River is approximately 0.5-0.66 m^3/s. In 2021, the averaged daily streamflow from August 15 to September 15 was 0.6 m^3/s, and in 2022 the averaged daily streamflow from September 15 to October 15 was 0.64 m^3/s. The above calculated groundwater seepage is very close (~100%) to the entire summer low flow recorded in those years. Although some of the parameters are subjective, it does indicate that during low flow season, groundwater is the primary source of base flow in the Upper Bulkley River.

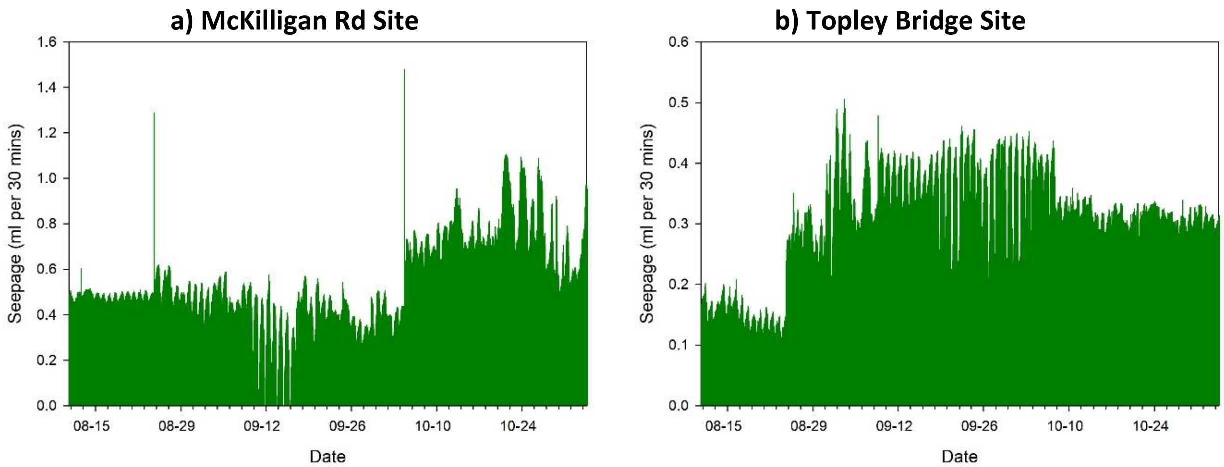

Figure 18: Calculated 30-minute integrated seepage rates at: a) McKilligan Rd site ($K=5\times10^{-8}$ m/sec), b) Topley bridge site ($K=3.33\times10^{-8}$ m/sec). Each bar represents the total seepage volume in 30-minute interval.

4.4 Drone Overflights and Thermal Imaging

A DJI Phantom 4 was used for drone overflights between 2018 and 2020. In 2021, a FLIR thermal imaging camera was mounted on the drone to capture surface water temperature profiles at a few selected locations in an attempt to identify groundwater seepage during the periods of pronounced temperature contrast between groundwater and surface water (e.g., Anibas et al., 2011). The purpose of the flights was to conduct watershed reconnaissance and guide field experiment site selection (e.g., in an area where groundwater seepage is prominent). In the watershed, however, the final site selections were largely restricted by the access to the sites, as well as the streambed material (e.g., relatively fine and soft sediment) to ensure proper seal of the cylindrical drum. Upon completion of the drone flights, the only point of convergence between reconnaissance findings and field installations was at the Topley Bridge site.

In this report, only the preliminary results of the drone overflights will be displayed and discussed. Future investigations will be undertaken to gain a full understanding of the application of thermal imaging on groundwater and surface water interactions.

Drone overflight and thermal imaging were conducted in a series of flights between 2018 and 2021. As discussed in Section 4.3, only the Topley Bridge site was selected as the result of the test flight. Because the field experiment was conducted one year after the flight, and the captured thermal infrared image did not overlap with the exact instrumentation location at the Topley Bridge site, water temperature calibration was not performed. The following orthomosaic map and the overlapped stream temperature map were captured at a location around 1.5 km downstream of the Topley Bridge site.

The timing of the thermal infrared image generation is critical to identify the temperature anomalies along the stream. In Figure 19, some portions of the stream were covered by ice, so the greatest temperature contrasts occurred between the ice-covered and ice-free sections of the river. When a section remained ice-covered, the infrared camera recorded only the temperature on the ice instead of the temperature of the water beneath. Open water observed along the straight section of the river may have resulted from two factors: 1) increased flow velocity that broke up ice earlier, and (2) groundwater recharge, which remained relatively steady through the year, and accelerated ice melting. The small open-water zone at the confluences of the two tributaries north of the main channel were unlikely to be explained by flow velocity alone given that the tributaries are small and remained mostly ice covered. Instead, it may reflect the combined influence of streamflow dynamics and warmer groundwater recharge.

Groundwater recharge to streams is more common along riverbanks where shallow groundwater flow paths intersect with the stream channel (e.g., Haynes et. al., 2022). Due to the shallow water depth and smaller flow velocity, it is not instantaneously mixed with the stream water in the main channel to diminish the groundwater temperature signature. In early spring when most of the banks are covered by snow and ice, the temperature anomalies are difficult to detect. In the future, summertime overflights may facilitate clearer identifications of groundwater upwelling locations.

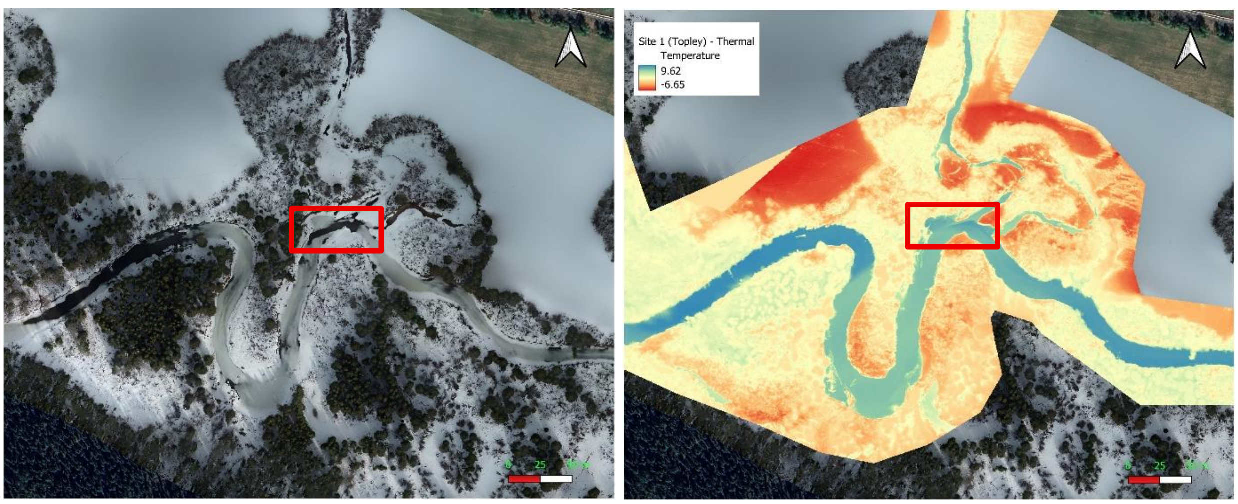

Figure 19: Orthomosaic and thermal map of a segment of the Upper Bulkley River. Displayed temperature is directly from the thermal camera with no calibration. The open-water section with slightly higher temperature shown in red squares may reflect the impact of the warmer groundwater recharge.

5. <u>CONCLUSION AND RECOMMENDATIONS</u>

In this study, three field investigation approaches were used to assess groundwater–surface water interactions in the Upper Bulkley River watershed: (1) water level and temperature monitoring in private wells, (2) direct measurement of groundwater seepage to the river, and (3) airborne thermal imaging.

Well monitoring is often used to assess aquifer conditions at regional scale (assuming sufficient spatial coverage), whereas direct recharge measurements are employed to evaluate groundwater contributions to streams at local scale. Airborne thermal imaging offers flexibility across spatial scales but is most often applied to stream segments ranging from a few hundred metres to several kilometres in length.

The results of the private well monitoring are consistent with our common understanding of hydraulic conductivity between aquifers and streams: unconfined alluvial aquifers are connected to the Upper Bulkley River and confined aquifers are less likely connected. The rapid recovery of the groundwater levels in response to the pumping, as well as the stable water levels in all the wells indicate that the connected aquifers during the observation period were relatively productive and not facing any imminent threat of depletion. Precipitation and spring snowmelt are the main recharge mechanisms.

The Upper Bulkley River is primarily fed by Bulkley Lake, but groundwater contributions sustain its baseflows as it moves downstream from the headwaters. With the current approach, the precise seepage to the stream is difficult to quantify given that the streambed hydraulic conductivity varies both spatially and temporally. Other factors such as the instrument accuracies impact the results as well. However, if enough spatial coverage is obtained, achieving the seepage quantity within one order of magnitude is possible. The results provide essential insight into the relative contributions of groundwater and surface water, particularly for informing water allocation decisions during low flow periods. They also underscore the importance of obtaining detailed streambed property data to more accurately characterize the degree of hydraulic connectivity. To better understand the seepage variabilities, more measurement locations or alternative methods would be required.

The results of the drone overflight are preliminary. More reliable results can be obtained when infrared thermal imagery is collected during the summer, when overall streamflow is low and the temperature contrast between groundwater and surface water reaches its maximum. However, the results did provide some insights on identifying potential discharge points using temperature anomalies.

Although well monitoring is largely dependent on the existing infrastructure (e.g., existing groundwater wells), future work to enhance our understanding of groundwater and surface water interaction could include:

1) Establish more seepage metre stations to understand the spatial variability of the groundwater recharge. Automated flow metres, if available, could largely enhance the efficiency of the work and increase the density of the seepage metre stations at one location. Other options such as fiber-optic distributed temperature sensing can also be used to improve the resolution of the monitoring.
2) Drill dedicated monitoring wells/boreholes through the surface sediments to delineate the vertical distribution of the sediment in and along the river channel.
3) Collect shallow cores of surface sediments to assess the physical linkage between the hyporheic zone and the underlying aquifers.
4) Conduct multiple drone flights during the summer to better capture the temperature anomalies. If the flights can be used to guide piezometer and seepage metre installation, the temperature can be calibrated to reflect the real temperature of the surface water and seeped groundwater. Because groundwater discharge tends be localized along preferential flow paths rather than being uniformly distributed, reconnaissance surveys are essential for identifying these zones.
5) Install additional hydrometric stations along the Upper Bulkley River to better characterize streamflow variability throughout the system.

REFERENCES

Anibas C., K. Buis, R. Verhoeven, P. Meire, and O. Batelaan. 2011. A simple thermal mapping method for seasonal spatial patterns of groundwater–surface water interaction, Journal of Hydrology, 397, 93-104, doi: 10.1016/j.jhydrol.2010.11.036

Cardenas, M. B. 2015. Hyporheic zone hydrologic science: A historical account of its emergence and a prospectus, Water Resources Research., 51, 3601–3616, doi:10.1002/2015WR017028.

Daly, C., M. Halbleib, J. I. Smith, W. P. Gibson, M. K. Doggett, G. H. Taylor, and J. Curtis. 2008. Physiographically sensitive mapping of temperature and precipitation across the conterminous United States. Int. J. Climatol., 28, 2031–2064

Domenico, P.A. and F.W. Schwartz. 1990. Physical and Chemical Hydrogeology, John Wiley & Sons, New York, 824 p

Genereux, D. P., S. Leahy, H. Mitasova, C. D. Kennedy, and D. R. Cobett. 2008. Spatial and temporal variability of streambed hydraulic conductivity in West Bear Creek, North Carolina, USA. Journal of Hydrology, 358, 332-353, doi: 10.1016/j.jhydrol.2008.06.017

Gribovszki, Z., J. Szilágyi, and P. Kalicz. 2010. Diurnal fluctuations in shallow groundwater levels and streamflow rates and their interpretation – A review. Journal of Hydrology, 385, 371-383, doi: 10.1016/j.jhydrol.2010.02.001

Haynes, A. B., M. A. Martin, E. Moore, K. Jackson, J. Knighton, D. M. Rey, and A. M. Helton. 2022. Shallow and local or deep and regional? Inferring source groundwater characteristics across mainstem riverbank discharge faces. Hydrological Processes, doi: 10.1002/hyp.14939

Hinnell, A. C., T. Lengyel, S. Funk, J. J. Clague and Z. M. Hammond. 2020. Vanderhoof and Houston Aquifer Mapping and Hydrostratigraphic Characterization. Water Science Series, WSS2020-07. Province of British Columbia, Victoria.

McLaughlin, D. L., and M. J. Cohen. 2011. Thermal artifacts in measurements of fine-scale water level variation, Water Resources. Research., 47, W09601, doi:10.1029/2010WR010288

Nitschke, C. R., M. Amoroso, K. D. Coates, and R. Astrup. 2012. The influence of climate change, site type, and disturbance on stand dynamics in northwest British Columbian, Canada, *Ecosphere*, DOI: 10.1890/ES11-00282.1

Rasmussen, T. C., and L. A. Crawford. 1997. Identifying and removing barometric pressure effects in confined and unconfined aquifers. Ground water, 35(3), 502-511.

Rosenberry, D. O., and J. Pitlick. 2009. Effects of sediment transport and seepage direction on hydraulic properties at the sediment–water interface of hyporheic settings. Journal of Hydrology, 373, 377-391, doi:10.1016/j.jhydrol.2009.04.030

Rosenberry, D. O., C. Duque, and D.R. Lee. 2020. History and evolution of seepage meters for quantifying flow between groundwater and surface water: Part 1 ‑ Freshwater settings. Earth-Science Reviews, https://doi.org/10.1016/j.earscirev.2020.103167

Rosenberry, D.O., E. Engesgaard, and C. Hatch. 2021. Hydraulic conductivity can no longer be considered a fixed property when quantifying flow between groundwater and surface water. Hydrological Processes, https://doi.org/10.1002/hyp.14226

Tian, F., and Z. Xu. 2024. Streamflow diurnal fluctuation and driving mechanism of headwater stream in a semi-humid mountainous region. Journal of Hydrology, https://doi.org/10.1016/j.jhydrol.2024.131803

Wang, T., A. Hamann., D. Spittlehouse and C. Carroll. 2016. Locally Downscaled and Spatially Customizable Climate Data for Historical and Future Periods for North America. PLoS ONE 11(6): e0156720. doi:10.1371/journal.pone.0156720

Westcott, B. 2022. Upper Bulkley River Watershed water temperature monitoring program 2016-21 data report. https://data.skeenasalmon.info/dataset/e0e8cb6b-1bc1-45d5-9d51-799c4c5d7d1e/resource/995cca24-a884-4a56-816f-37991378d652/download/ubrwatertemperaturedatasummary2016-21_final.pdf

Woessner, W. W. 2020. Groundwater-Surface Water Exchange: Rivers, Lakes, and Wetlands. The Groundwater Project. https://10.21083/978-1-7770541-5-1

Wondzell, S. M. 2006. Effect of morphology and discharge on hyporheic exchange flows in two small streams in the Cascade Mountains of Oregon, USA. Hydrol. Process., 20, 267–287, doi: 10.1002/hyp.5902.

Wroblicky, G.J., M. E. Campana, H. M. Valett, and C. N. Dahm. 1998. Seasonal variation in surface-subsurface water exchange and lateral hyporheic area of two stream-aquifer systems. Water Resources Research 34: 317-328.